Nonequilibrium Interlayer Transport in Pulsed Laser Deposition

J. Z. Tischler,[1] Gyula Eres,[1,*] B. C. Larson,[1] Christopher M. Rouleau,[1] P. Zschack,[2] and Douglas H. Lowndes[1]

[1]*Condensed Matter Sciences Division, Oak Ridge National Laboratory, Oak Ridge, Tennessee 37831, USA*

[2]*Frederick Seitz Materials Research Laboratory, University of Illinois, Urbana, Illinois 61801, USA*

(Received 28 February 2006; published 6 June 2006)

We use time-resolved surface x-ray diffraction measurements with microsecond range resolution to study the growth kinetics of pulsed laser deposited $SrTiO_3$. Time-dependent surface coverages corresponding to single laser shots were determined directly from crystal truncation rod intensity transients. Analysis of surface coverage evolution shows that extremely fast nonequilibrium interlayer transport, which occurs concurrently with the arrival of the laser plume, dominates the deposition process. A much smaller fraction of material, which is governed by the dwell time between successive laser shots, is transferred by slow, thermally driven interlayer transport processes.

DOI: 10.1103/PhysRevLett.96.226104 PACS numbers: 68.55.−a, 61.10.Nz, 81.15.Fg

Experimental simplicity and a high degree of control over deposition parameters make pulsed laser deposition (PLD) the method of choice for synthesis of a variety of complex and artificially structured materials [1,2]. The surface smoothness associated with PLD is particularly important in epitaxial engineering of perovskite-type metal oxide superlattices [3].

Film growth in PLD occurs from an energetic plume of material that is ejected from a solid target by pulsed laser ablation. The plume consists of a complex mixture of neutral and ionized atoms, molecules, and small clusters with kinetic energies ranging from thermal to a few hundred eV [1,4]. The pulsed mode of deposition and the transient enhancement of surface mobility are key characteristics that differentiate PLD from thermal equilibrium deposition techniques such as molecular beam epitaxy (MBE) [5,6]. Simulations and modeling suggest that simple modulation (or chopping) of the continuous incident flux in MBE can have profound effects on two-dimensional (2D) film growth [5]. The presence of both energy-enhancement and pulsed deposition in PLD provides an even richer environment for exploration. Calculations for pulsed deposition predict new scaling relationships and the emergence of new growth regimes with the potential to tailor surface morphology and the properties of films using PLD [6].

Although, investigations of PLD have varied laser pulse rates [7], and qualitative assessments have been made of the effects of energy enhancement on the surface morphology [8,9], the evolution of the very high, instantaneous flux densities, and the nonequilibrium inter- and intralayer migration and aggregation processes on the growing surface [10] during thermalization have not been studied.

Diffraction techniques are particularly well suited for epitaxial growth-kinetics studies because they provide surface-specific, real-time information on the formation of crystalline structure [11]. Both reflection high-energy electron diffraction (RHEED) [12–14] and surface x-ray diffraction (SXRD) [15–17] have been used in studies of $SrTiO_3$ PLD. In contrast to the much harder to quantify step-edge densities used in RHEED [11,18], x-ray diffraction allows the use of the kinematic approximation to perform quantitative intensity analysis [19,20] in terms of layer coverages. In this Letter we report the use of time-resolved SXRD measurements with microsecond range resolution. We show by direct analysis of SXRD intensity transients for individual laser shots that nonequilibrium intra- and interlayer transport (during the thermalization of the laser plume on the growing surface) is the dominant growth process, and further that it occurs on a time scale at least 3 orders of magnitude faster than the thermal equilibrium transport processes that follow.

The measurements were performed on the UNICAT undulator beam line at the advanced photon source using a monochromatic 10 keV x-ray beam and an *in situ* PLD chamber described in a previous publication [15]. The diffracted intensity was measured at the specular $(0\,0\,\frac{1}{2})$ anti-Bragg reflection using an avalanche photodiode detector. The as-received samples were etched in a buffered HF solution with a $p\mathrm{H} \sim 5$ for 60 s and annealed at temperatures in a range from 950 to 1050 °C. The annealed substrates were imaged by atomic force microscopy (AFM) and samples with well-developed terraces were selected for the growth experiments. Following a preanneal step in 2 mTorr of oxygen background at 850 °C, the specular rod intensity stabilized around 8×10^5 cps at the growth temperature of 650 °C.

The $(0\,0\,\frac{1}{2})$ SXRD transients in Fig. 1 illustrate the response of the growing surface starting before the arrival of the laser plume through the dwell time between successive laser pulses during which no deposition occurs. The discontinuous drop and jump in Fig. 1 correspond to the arrival of the laser plume at the growing surface and indicate that $SrTiO_3$ unit cell formation (crystallization) occurs faster than our fastest sampling time of 6 μs (binned to 25 μs). Therefore, this time scale represents an upper bound for the time scale for the energetic plume species to thermalize and aggregate into crystal lattice

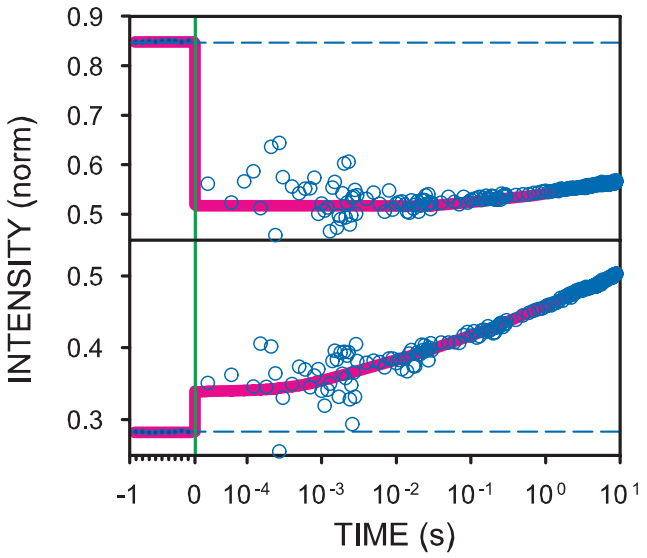

FIG. 1 (color). $(0\,0\,\frac{1}{2})$ SXRD transients for 10 s dwell time measured with 6 μs sampling time and binned to 25 μs. The drop (upper half) corresponds to the second laser shot after the growth oscillation maximum, and the jump (lower half) corresponds to the second shot after the growth oscillation minimum. The data are averaged over 10 shots. The horizontal dashed lines designate the intensity before the laser shot and the vertical green line designates when the laser was fired. The thick lines are guides to the eye. Note that the statistical fluctuations in the data decrease with time because a logarithmic sampling time scale was used for data collection after the laser shot.

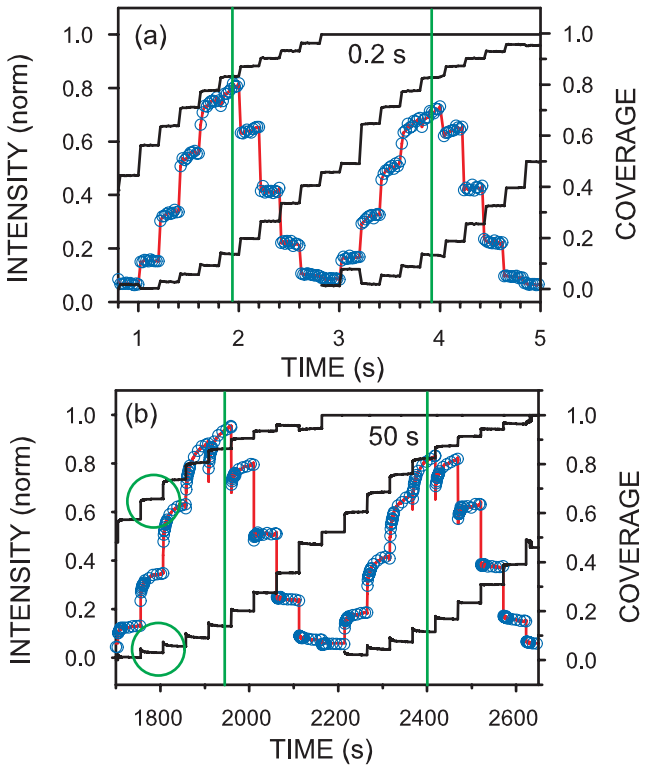

FIG. 2 (color). $(0\,0\,\frac{1}{2})$ SXRD growth oscillations; (a) 0.2 s dwell time, (b) 50 s dwell time. The measured SXRD intensity transients are shown by the overlapping blue circles and the red lines represent the calculated intensity. Layer coverages are shown in black. The green lines and circles represent markings explained in the text.

sites. This is comparable to the plume arrival time that lasts for 2–10 μs [4,21]. Because of limited time resolution, previous RHEED [12–14] and SXRD [15–17] studies observed only the slow component of the intensity transients after thermalization of the laser plume and thus constructed an incomplete picture of $SrTiO_3$ growth kinetics.

To investigate the fast (nonequilibrium) and the slow (thermal) steps in $SrTiO_3$ PLD, we have made a detailed study of SXRD transients for dwell times that varied by a factor of 250. The measurements in Fig. 2 show that the intensity oscillations of SXRD transients follow the familiar parabolic shape of RHEED oscillations. Under optimal growth conditions, these oscillations persist indefinitely [15]. Although the transients for 0.2 s and 50 s dwell time appear self-similar, closer examination reveals that the intensity jumps and the shape of the SXRD transients exhibit a distinct dependence on the layer coverage and the dwell time.

Rather than fitting the data to transport models [22], we instead analyze the intensity transients using an approach that allows direct determination of surface coverages from the diffracted intensities, without assumptions about the physics of the underlying growth process. This approach and its validity are driven by roughness analyses using AFM images of the substrates before growth and the films after growth. Analysis of a large number of AFM images of films of different thicknesses grown under a wide range of conditions shows that the roughness, even after more than 100 layer deposition, is limited to only two layers. Examples of such AFM images are shown in Fig. 3. This simple but powerful result implies that the growth interface width can be no more than two layers at any time during growth, and consequently a ''two-layer'' coverage model can be used to analyze our SXRD measurements.

Accordingly, we have performed a quantitative analysis of the SXRD measurements of PLD growth in Fig. 2 using the following two-layer form of the kinematic intensity: $I(t) = I_0[(1 - 2\theta_n(t) + 2\theta_{n+1}(t))]^2$ [18,22], where I_0 scales the incident intensity and $\theta_n(t)$ and $\theta_{n+1}(t)$ represent the fractional coverages of the growing layer (layer n) and islands on the growing layer (layer $n + 1$), respectively, for each measurement time, t. Note that with the constraint of $\theta_n(t) + \theta_{n+1}(t) =$ deposition per pulse and a single I_0, the coverages $\theta_n(t)$ and $\theta_{n+1}(t)$ are the solution of the above equation for $I(t)$ at each measuring point. In Fig. 2 the overlapping blue circles represent the measured SXRD intensity transients, the red line represents the calculated intensity, and the black solid lines show the corresponding layer coverages. The steps in the intensity and the coverage

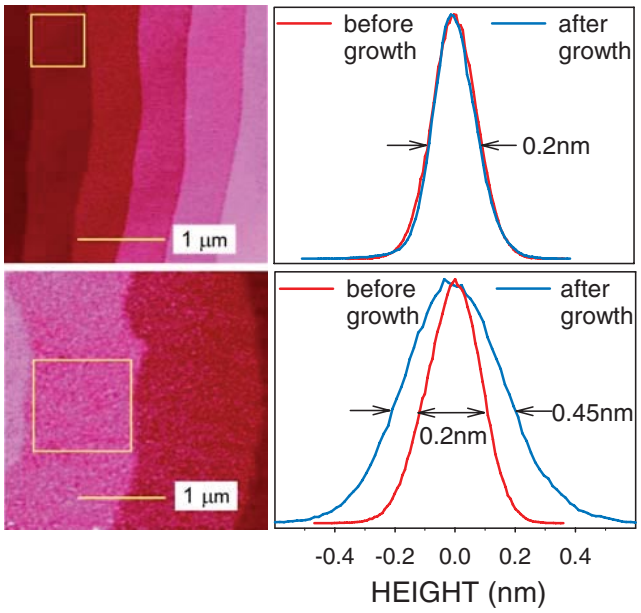

FIG. 3 (color). Example of smooth (top row) and slightly rough (bottom row) growth. AFM images, and surface height histograms before (red line) and after (blue line) growth of more than one-hundred unit cell thick $SrTiO_3$ films at 2 s (top) and 50 s (bottom) dwell time. The histogram data were obtained from single terraces as shown by the yellow squares in the AFM images.

data correspond to individual laser shots. Complete filling at oscillation maximum would correspond to the hypothetical plot in Fig. 4(a), which requires infinitely fast interlayer transport and the absence of islands on top of the growing surface (i.e., $\theta_{n+1} = 0$). In contrast, the vertical green lines in Fig. 2 show that at real intensity maxima layer coverage is only ~0.85 and that θ_{n+1} is already more than 0.1 for both long and short dwell times. As a result, we see that growth occurs on two layers over two oscillations and that layers have ~50%–60% island coverage at their completion. As layer coverages in Figs. 2(a) and 2(b) illustrate, layer filling continues after the maximum and the majority of layer growth (~70%) for a particular layer occurs between successive maxima, but neither nucleation nor completion of the layers coincide with intensity maxima.

While overlapping layer growth identified by the layer coverage in Fig. 2 is not a new concept, the ability to make a direct determination of when island nucleation commences on top of the growing layer and when hole filling is complete within the growing layer is new. We emphasize that the growth mode within any particular layer is essentially layer-by-layer (LBL) growth in the sense that growth commences with island nucleation, continues with island growth until the islands coalesce, and then proceeds with hole filling until the layer is complete.

We comment that these results are consistent with computational expectations regarding nucleation and interisland distance distribution associated with the very high instantaneous fluxes of PLD [6]. They are in accord with the absence of a step-edge barrier [15] in $SrTiO_3$ as well, in the sense that nucleation of new islands does not occur until coalescence is reached [23]. At coalescence, island merging rapidly transforms the surface into a single interconnected layer with holes, on which new island nucleation becomes inevitable above the percolation threshold $\theta_p > \sim 0.6$ coverage [23]. The significance of θ_p is that at this coverage the islands reach the size necessary for the nucleation of new islands on the growing layer [24]. Our observations are consistent with theoretical studies of island growth, coalescence, and percolation trends by Amar *et al.* which show that the percolation threshold occurs in the range from $\theta_p = 0.593$ to 0.785 [24].

The most important and completely new type of information obtained from the transient intensity analysis is contained in the time-dependence of the individual coverage profiles in Figs. 2 and 4(b). The initial change in the coverages shows the fraction of the deposited pulse forming instantaneously on each layer, and the time evolution of the coverages shows the amount transferred from the island

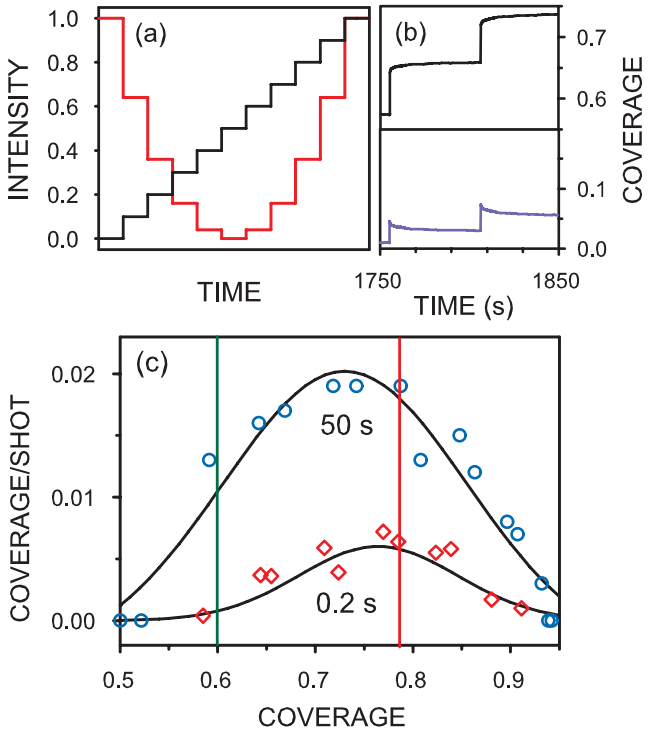

FIG. 4 (color). (a) A model plot for one period of perfect LBL growth using 10 shots per layer. The intensity is given by the red and the coverage by the black line. (b) Magnified plot of layer coverages for the circled laser shots in Fig. 2(b). (c) The fraction of material transferred by the slow interlayer transport step at 0.2 s dwell time (red diamonds) and 50 s dwell time (blue circles). The solid lines are Gaussian fits to the experimental data. The vertical lines illustrate the coverage for ordinary site percolation [$\theta_p = 0.593$, green, Ref. [24]], and island coalescence on a square lattice [$\theta_p = 0.785$, red, Ref. [24]].

(top) layer [blue line in Fig. 4(b)] to the growing (bottom) layer [black line in Fig. 4(b)] during the dwell time. The enlarged view of coverage evolution in Fig. 4(b) shows qualitatively that most of the deposited pulse reaches the bottom layer during the instantaneous, nonequilibrium phase of the surface evolution (i.e., during the thermalization process) and that only a relatively small amount is transferred by thermal equilibrium processes. Since we showed in Fig. 1 that the time scale for the instantaneous, energy-enhanced interlayer transfer is on the order of microseconds or less, and quite distinct from the much slower thermal equilibrium component, we have direct evidence that nonequilibrium processes dominate PLD growth.

The thermal component of the interlayer transport (per deposition pulse) is plotted in Fig. 4(c) for all coverages for which it is significant for both short and long dwell times. This figure shows that the maximum thermally transferred fraction is only 20% for 50 s (i.e., 0.02/0.1) and even less, 5%, for 0.2 s dwell time. It also shows that thermal equilibrium interlayer transfer is significant only for growing layer coverages above $\sim$0.6, where nucleation of the new layer begins. This result is fundamentally important. It shows directly that PLD growth takes place primarily by extremely fast, nonequilibrium processes. Moreover, the 4 times smaller thermal equilibrium fraction for the 0.2 s dwell time shows that the sluggish thermal transport component, which has been attributed to various processes including surface diffusion, crystallization, or surface rearrangement [12–17], can be minimized by the use of shorter dwell times. The overlapping LBL growth mode enables more effective layer completion using fast laser-driven nonequilibrium transport instead of slow thermal interlayer transport that requires relatively long dwell times during which thermal ripening processes dominate and cause degradation of surface morphology [15–17].

In summary, we have made time-resolved SXRD measurements on the microsecond scale, and two-layer film growth analyses of homoepitaxial PLD growth of $SrTiO_3$ that provide new insight into the growth processes associated with PLD. Specifically, we have shown that PLD film growth is dominated by fast, nonequilibrium processes that occur during thermalization of the laser plume on the growing surface. In addition, we have shown that much slower, thermally driven processes that occur during the dwell time play a relatively minor role in interlayer transport and can be further reduced by the use of shorter dwell times.

Research sponsored by the Division of Materials Sciences and Engineering, Office of Basic Energy Sciences, US Department of Energy, under Contract No. DE-AC05-00OR22725 with Oak Ridge National Laboratory, managed and operated by UT-Battelle, LLC. The UNICAT facility is supported by the US DOE through the Frederick Seitz Materials Research Laboratory at the University of Illinois at Urbana-Champaign, the Oak Ridge National Laboratory, the National Institute of Standards and Technology, and UOP LLC. The APS and the Center for Nanoscale Materials are supported by the US DOE, Basic Energy Sciences, Office of Science.

*Electronic address: eresg@ornl.gov

[1] D. H. Lowndes *et al.*, Science **273**, 898 (1996).
[2] P. R. Willmott, Prog. Surf. Sci. **76**, 163 (2004).
[3] H. N. Lee *et al.*, Nature (London) **433**, 395 (2005).
[4] D. B. Chrisey and G. K. Hubler, *Pulsed Laser Deposition of Thin Films* (Wiley, New York, 1994).
[5] N. Combe and P. Jensen, Phys. Rev. B **57**, 15 553 (1998).
[6] B. Hinnemann, H. Hinrichsen, and D. E. Wolf, Phys. Rev. E **67**, 011602 (2003).
[7] G. Koster *et al.*, Appl. Phys. Lett. **74**, 3729 (1999).
[8] P.-O. Jubert, O. Frushart, and C. Meyer, Surf. Sci. **522**, 8 (2003).
[9] H. Jenniches *et al.*, Appl. Phys. Lett. **69**, 3339 (1996).
[10] Z. Zhang and M. G. Lagally, Science **276**, 377 (1997).
[11] M. G. Lagally, D. E. Savage, and M. C. Tringides, in *Reflection High-Energy Electron Diffraction and Reflection Electron Imaging of Surfaces*, edited by P. K. Larsen and P. J. Dobson (Plenum, New York, 1988), p. 138.
[12] M. Y. Chern *et al.*, J. Vac. Sci. Technol. A **11**, 637 (1993).
[13] D. H. A. Blank *et al.*, Appl. Surf. Sci. **138–139**, 17 (1999).
[14] M. Lippmaa *et al.*, Appl. Phys. Lett. **76**, 2439 (2000).
[15] G. Eres *et al.*, Appl. Phys. Lett. **80**, 3379 (2002).
[16] A. Fleet *et al.*, Phys. Rev. Lett. **94**, 036102 (2005).
[17] A. Fleet *et al.*, Phys. Rev. Lett. **96**, 055508 (2006).
[18] A. Ichimiya and P. I. Cohen, *Reflection High Energy Electron Diffraction* (Cambridge University Press, Cambridge, England, 2004).
[19] R. Fiedenhans'l, Surf. Sci. Rep. **10**, 105 (1989).
[20] E. Vlieg, Surf. Sci. **500**, 458 (2002).
[21] Y. Franghiadakis, C. Fotakis, and P. Tzanetakis, Appl. Phys. A **68**, 391 (1999).
[22] P. I. Cohen *et al.*, Surf. Sci. **216**, 222 (1989).
[23] G. Rosenfeld, B. Poelsema, and G. Comsa, in *Growth and Properties of Ultrathin Epitaxial Layers*, edited by D. A. King and D. P. Woodruff (Elsevier, New York, 1997), p. 66.
[24] J. G. Amar, F. Family, and P.-M. Lam, Phys. Rev. B **50**, 8781 (1994).